Thermal Cycling Impact on Supercapacitor Performance and Leakage Current under Constant Voltage Test

Mohamed Ayadi [a,b *], Olivier Briat [a], Gérard Coquery [b], Jean-Michel Vinassa [a]

[a] Université de Bordeaux, IMS, UMR CNRS 5218, Talence, F-33405, France
[b] IFSTTAR Satory, Laboratoire des Technologies Nouvelles, Versailles, F-78000, France
* E-mail : mohamed.ayadi@ims-bordeaux.fr

***Abstract* - In this paper, we present a comparative study that focus on Supercapacitor (SC) thermal cycling and calendar ageing under constant voltage tests. The impacts of cycling temperature on SC performance and degradation rate are studied. Obtained results from thermal cycling ageing test are compared with those coming from simple calendar ageing test at constant voltage and constant temperature. The comparison method used is based on physics modelling parameters evolution in the Multi-Pore (MP) and the Constant Phase Element (CPE) models. Parameters are calculated based on experimental measurements results up to 13000 h of ageing test. The impact of thermal cycling during ageing tests on the measured leakage current is also presented.**

I. INTRODUCTION

Supercapacitors (SC), or Electric Double-Layer Capacitors (EDLC) are based on the electrostatic storage of the energy at the interface between a porous carbon electrode and an electrolyte. Due to their low impedance and high capacitance, SCs are well suited for energy buffer applications that need a high pulse current capability or a large storage capacitance [1]. SCs are considered as one of the potential devices for energy recovery in Hybrid Electric Vehicles (HEV) application because of their high power capability (between 5 and 15 kW kg^{-1}). Classic storage element in HEV consists in accumulators, which allow a relatively high autonomy. However, the power capability of these devices can be considered as insufficient. SCs are promising storage systems used in these applications to minimize this lack thanks to their ability to provide high level of power and current [2]. The understanding of the ageing mechanisms and the development of new characterization methods are the main remaining challenges for SCs [3]. In addition to the power cycling ageing mode, their performances decrease in terms of energy and power capabilities during rest time [4]. This ageing mode is well known as calendar mode [5].

One of the ageing causes for SCs in HEV applications is the day/night cycling, that is why we study the impact of thermal cycling on SC performances in this paper. This article deals with the impact of thermal cycling on SC performances by comparing ageing mechanisms with those observed in simple calendar ageing tests. Two kind of model based on physical description of the porous structure, CPE and MP, are used to study the internal structure evolutions during ageing for the both ageing tests. In addition, a comparison method based on parameters modelling study is used to show internal physical parameters change between the two kinds of tests. The impacts of thermal cycling on SC measured leakage current are also highlighted.

II. SUPERCAPACITORS CHARACTERIZATIONS METHODS

To quantify the evolution of SCs performances in terms of capacitance (C) and Equivalent Series Resistance (ESR), a monitoring of ageing process with periodic characterization tests are made. For this, we analyze SCs performances, C and ESR, in both frequency (AC) and time domains (DC). Impedance measurements, AC or DC, are used habitually to characterize degradation tendency of SCs. The internal resistance of SCs consists mainly of the resistances of electrolyte and porous activated carbon electrode [6]. The AC impedance measurement can separate these two parts, while the DC measurement determines only the sum of the both [7].

For AC characterization, the existing impedance analyzers allow the examination of a frequency range among a few of µHz to MHz. In our case, for Electrochemical Impedance Spectroscopy (EIS) tests we use a Zahner IM6 impedance analyzer with a PP240 power booster. With this electrochemical workstation, the impedance measurement is made in the interval [10 mHz; 1kHz] which is more adapted to the use of SCs in HEV application because the power pulse required in this case will have their frequency spectrum inside this interval [8].

Then, in case of DC characterization, constant current tests represent a characterization method that is useful to track the performance state of SCs by monitoring C and ESR evolution. An application of a method based on the IEC62576 standard is used by applying a constant charging and discharging current on SC. Fig. 1 show the DC characterization that we have used in ours tests.

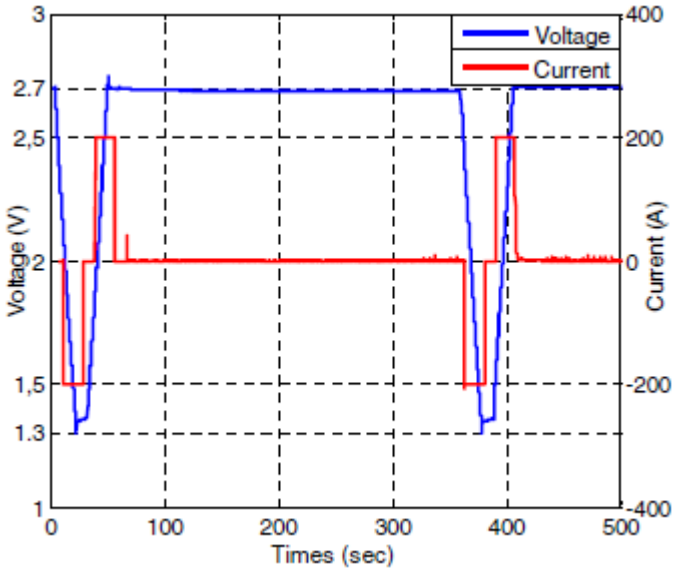

Fig. 1. Time domain characterization method of SC.

III. CONSTANT VOLTAGE AGEING TESTS

Ageing tests have been done on 3000 F SCs cells with acetonitrile based electrolyte and having 2.7 V as nominal voltage. We will focus on two categories of ageing types. The first one is the simple calendar ageing, the second is the thermal cycling ageing test: calendar ageing with a periodic temperature variation between two constant values. According to obtained results coming from these tests, we will study the influence and the impact of them on the rate degradation of SCs performances and the leakage current evolutions.

A. Simple Calendar Ageing Test

SCs are aged at constant voltages and temperatures in this test. During calendar ageing, SCs are placed inside a climatic chamber in order to attain device thermal control. In this study, SCs have been tested with different temperatures and one constant voltage value. Temperature values that have been selected are (40, 50 and 60°C) and the voltage is fixed at 2.8V. The stability range of the electrolyte limits the maximum operating voltage of the SC and, in our case; the tested cells have a nominal operating voltage of 2.7V. In fact, these values of voltages and temperatures are selected in order to accelerate the rate of ageing mechanism [9]. We notice that only results of 50°C will be presented for this kind of test in this paper and that the leakage current have been measured during all the tests duration.

B. Thermal Cycling Test

In this case, SCs are aged at constant voltage with a variable temperature, the temperature was not fixed during the whole test and it moves between two limits. Thermal cycling corresponds to a two steps profile with a temperature change period of two weeks and a changing ratio of 50%. In fact, one of SCs constraints for HEV application is the temperature switch (day / night) and that is why we study the impact of thermal cycling. The SCs voltage in this test are maintained also at 2.8V thanks to similar floating tools than in the simple calendar ageing tests and the leakage current is also measured during the total tests duration. Two profiles with two-steps are defined, [40°C - 50°C] and [40°C - 60°C]. During the whole experiment, SCs are placed inside a programmable climatic chamber in order to control the slope and the periodic change of the working temperature.

In our study, selected values of temperature and voltage have been considered in order to compare the obtained results with those issued from the simple calendar ageing tests. In addition, the floating test bench is used to precisely measure the resulting leakage current.

Characterization tests are done periodically in both frequency and time domains for these two ageing tests. We have to notice that all characterizations for thermal cycling tests are made always at the low temperature ie. 40°C (for 40-50°C and 40-60°C tests) because the ageing tests have been started at this low temperature and the first characterization points are obtained

in these conditions. We notice that the imaginary part of the measured impedance (thus the capacitance) does not depend on the temperature under which the characterization is made. Just a slight dependency is shown in the real part that decreases with temperature rise. To avoid differences that can take place when comparing results coming from different characterization temperatures, we use relative data (referring to initially measured data) and not absolute ones.

IV. MEASURED LEAKAGE CURRENT

A. Leakage Current Results for Ageing Tests

In our work, we focused on the measuring floating current, which corresponds to the current absorbed by the SC in order to maintain a constant voltage during ageing tests. An electronic board allowing a high measurement precision and a good continuous regulation of current is used for all our tests. The comportment of this current depends of the chemical mechanism shown on the storage systems according to their types (type of electrode and separator also), voltages and temperatures. In the case of electrolytic or dielectric capacitors, the voltage drop that occurs is due to the leakage current that flow between electrodes, without any chemical processes. This current is the leakage current flowing through a resistance present between electrodes, due to the undesired imperfection of insulating materials used in the device [10]. In the case of EDLC (SCs), in addition to this leakage current type, which is present between SC electrodes through the isolator, a part of absorbed floating current is due to faradic charge transfer reactions caused by local overcharging or impurities in activated carbon structure.

Results of obtained measured floating current confirm that we have two parts in the current curve: a part with a fast decrease of absorbed current and a second one with a nearly constant current as we can see in Fig. 2. The first part of the measured leakage current is generally composed of two factors: an ionic current and a part of electronic current that still present partly in the second part. This current, the second part, would remain nearly constant [11].

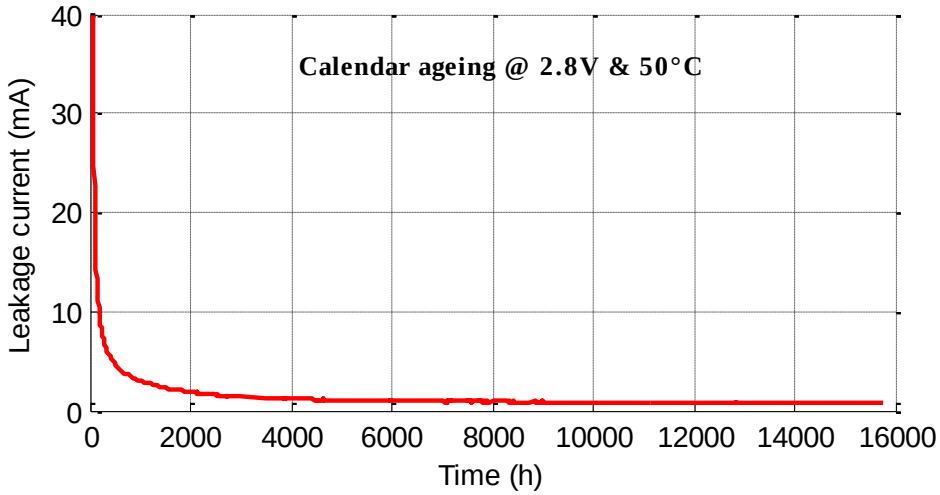

Fig. 2 . Evolution of floating current for the simple calendar ageing test @50°C & 2.8V.

Results of measured leakage current for different thermal cycling ageing tests (40/50°C and 40/60°C under 2.8V) are presented in Fig.3 with the obtained current for calendar ageing test (50°C & 2.8V). These results show that leakage current does not stay at a constant value in the case of thermal cycling tests. This current is clearly depending of the applied temperature and it change value every time the temperature change. Also, as we can see, the mean value of the SC leakage current in thermal cycling 40/50°C is a little lower than the leakage current corresponding to calendar ageing @50°C. Moreover, if we look for the 40/60°C results, we can clearly say that its mean value is more important than the calendar ageing leakage current at the mean value of the test temperatures (50°C). Therefore, we can conclude that the thermal cycling ageing stress at 40/60°C is more important compared to the resulting stress of the mean temperature value (50°C) and at the same voltage of tests (2.8V).

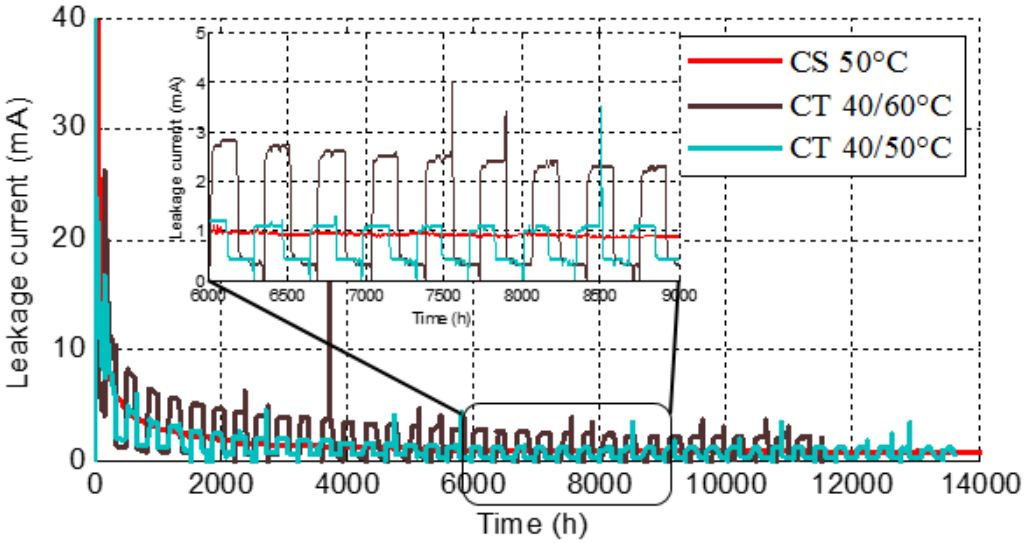

Fig.3 .Evolution of floating current for simple calendar and thermal cycling-ageing tests @50°C & 2.8V; 40/60°C &2.8V and 40/50°C &2.8V.

B. Temperature Effects on Measured Leakage Current

A temperature increase on SC under calendar ageing test, conduct to a rise on absorbed leakage current. This behavior justifies the acceleration of self-discharge observed at high temperature [4]. As we can see in Fig.4, an example of decrease of temperature from 50 to 40°C cause a decrease in leakage current because the constrains at the first thermal state are more important from those at the second one, so the needed leakage current value is lower at 40°C than at 50°C. However, if we look more closely, we can observe that we have an increase during a short time before reaching the lowest value (transitory state). This variation is the result of a slight variation of voltage for both increasing and decreasing temperature. We can explain this as a transition phase between two equilibriums states caused by the dependency of voltage and internal impedance with temperature [12].

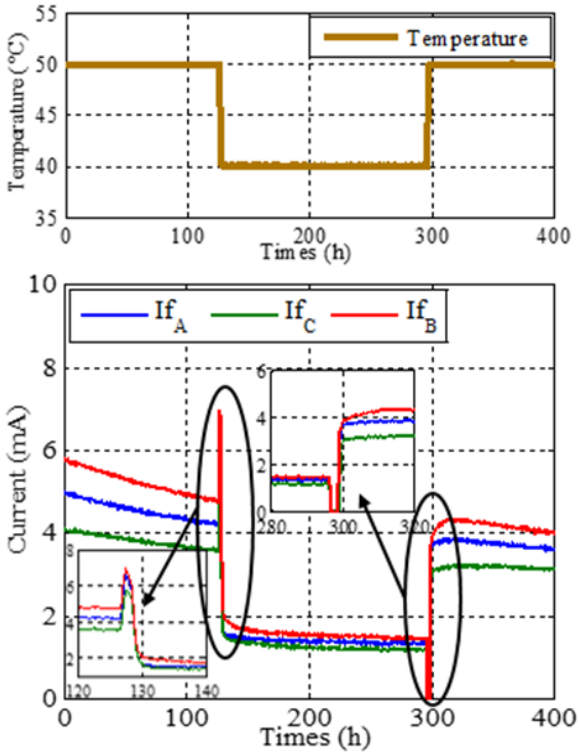

Fig. 4 Leakage current variation under temperature change during calendar ageing

V. SUPERCAPACITORS MODELLING

The dynamic behavior of a SC is strongly related to the ions mobility, the used electrolyte and to the porosity effects and nature of the porous electrodes, which is considered as one of the main internal characteristics of SC [13]. Because of their high porosity, we observe different kinetic effects from those detected in a conventional planar electrode, so we get a strong influence on the cell impedance. For this reason, a simple *RC* series circuit does not allow obtaining of a correct modelling of the SCs dynamic behavior in a wide frequency range. Consequently, in this paper, we used impedance models based on physical description of the porous structure.

The general equivalent model of a SC is presented in Fig. 5 (a). In this case, a series resistor (R_s), an inductor (L_s) and a complex pore impedance (Z_p) present the SC.

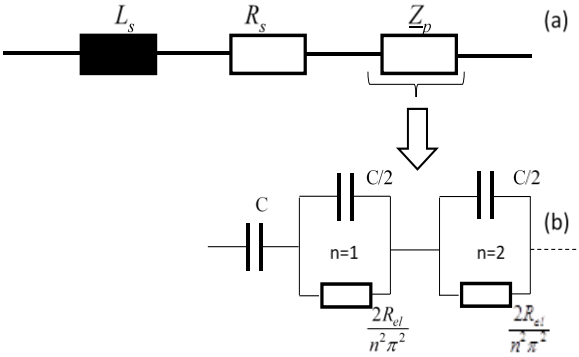

Fig. 5. (a) Equivalent circuit of a Supercapacitors; (b) equivalent electric circuit of pore impedance

We have to notice that the inductive behavior is not very attentive for SCs applications. In our case, the use of an inductor in this model is just to avoid modeling errors that could influence the estimation of series resistance R_s in the middle frequency branch of the spectrum. The impedance Z_p models the porosity of the SC. The mathematical expression of Z_p *(jω)* is given by equation (1) with $\tau = \sqrt{R.C}$; *C* and *R* present the total electrode capacitance and resistance respectively.

$$\underline{Z}_p(\mathrm{j}\omega) = \frac{\tau.\coth(\sqrt{\mathrm{j}\omega\tau})}{C.\sqrt{j\omega\tau}} \tag{1}$$

The equivalent electric circuit of (Z_p) includes a series of N *RC* parallel branches (Fig. 5 (b)) representing the charge diffusion in the porous structure which correspond to a series expansion of the transmission line model [14]. To be more accurate and because of the correspondence of double layer charge process to an imperfect capacitor more than a perfect one, we use a Constant Phase Element (CPE) to model this imperfect capacitor as can be showed in Fig. 6.

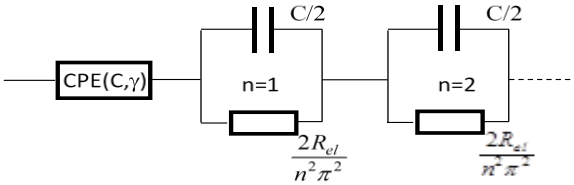

Fig. 6. Equivalent circuit for CPE model.

The impedance of this CPE is given by equation (2) where A is the magnitude and (1-γ) is the exponent with γ is a parameter whose value ranges from 0 to 1. This parameter is used to take into account the slow phenomena.

$$Z_{cf} = \frac{1}{A.(j\omega)^{(1-\gamma)}} \tag{2}$$

Then, the expression of the cell impedance can be expressed as given in equation (3) where the resistance R_{el} is mainly depends on the electrolyte conductivity inside porous structure.

$$Z_t = R_S + \sqrt{\frac{R_{el}}{(j\omega)^{(1-\gamma)}C}}.\coth(\sqrt{(j\omega)^{(1-\gamma)}R_{el}.C}) + L_S \tag{3}$$

Indeed, industrial porous electrode building process implies necessarily a geometrical dispersion of pore sizes. To solve this problem, the CPE model was developed previously, but to differentiate between different pores behavior, Multi-Pore (MP) model can be used. This model was developed by Hammar [15] and his idea was to model each group of pores by a branch, so each group of pores have the same individual impedance characteristics (R_{eli}, C_{dli}). The impedance of the wholly porous structure is obtained by the parallelization of branches as shown in Fig. 7.

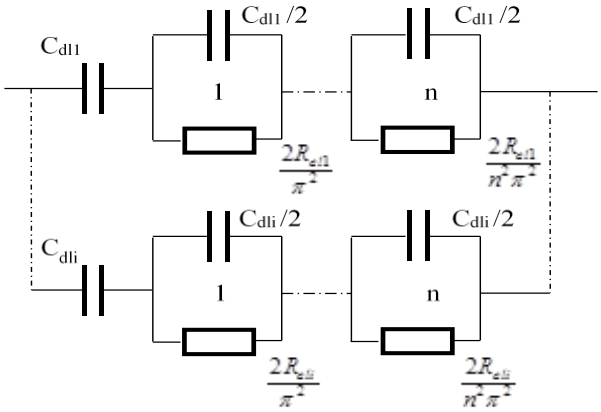

Fig. 7. Equivalent electrical circuit of a porous structure impedance for MP model.

Therefore, the total impedance of porous structure is obtained by the parallelization of Z_p as expressed in equation (4) with $\tau_i = \sqrt{R_{eli}.C_{dli}}$.

$$\underline{Z}_{TotalStructure}(j\omega) = \frac{\tau_1.\coth(\sqrt{j\omega\tau_1})}{C_{dl1}.\sqrt{j\omega\tau_1}} // \ldots \frac{\tau_i.\coth(\sqrt{j\omega\tau_i})}{C_{dli}.\sqrt{j\omega\tau_i}} \quad (4)$$

Fig. 8 show an example of validation of used models in the range frequency of [10 mHz; 1kHz]. The evolution of the real part of cell impedance and capacitance with frequency are presented in Fig.8 (a) and Fig.8 (b) respectively. We obtain a good estimation of measured results with modelling and the differences between simulated and measured parameters are very slight.

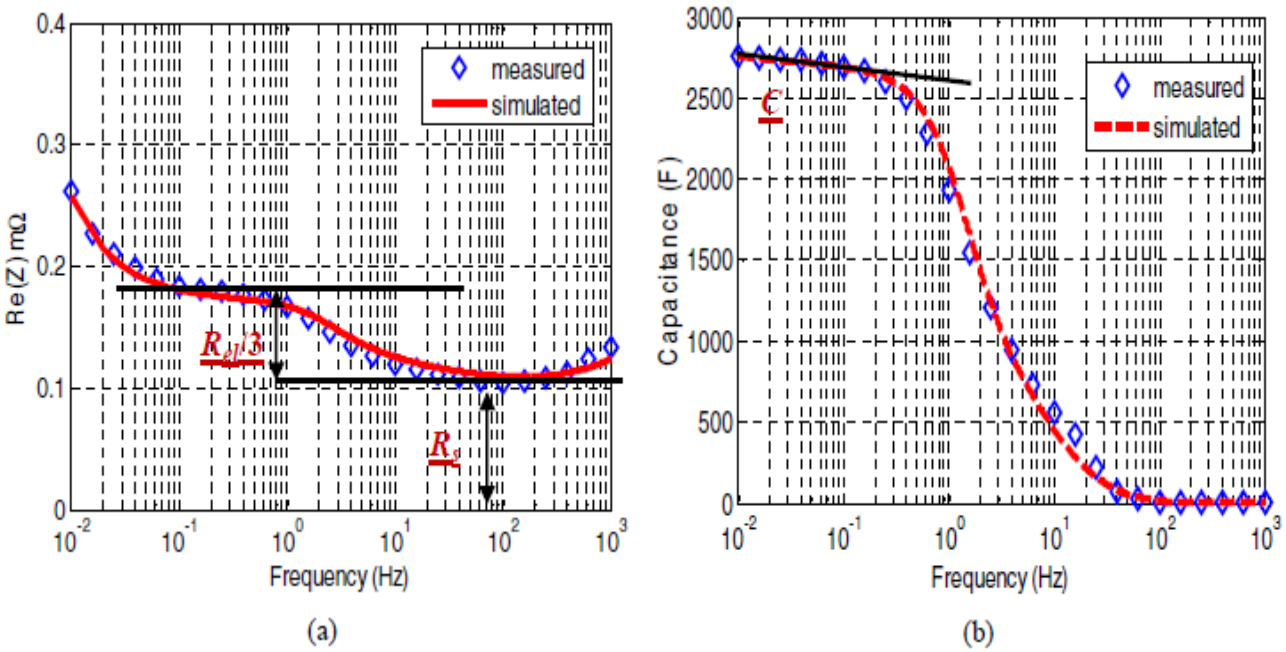

Fig.8. Comparison between simulated and calculated parameters of a 3000F SC.

VI. AGEING TESTS AND MODELLING RESULTS

A. Calendar and Thermal cycling Ageing Tests Results

We present in this first part obtained results showing the evolution of the capacitance and ESR of SCs with calendar ageing. The ESR is calculated from the impedance real part at 100mHz and the capacitance is calculated from the imaginary part at 10mHz. These frequency values are confirmed by manufacturer datasheet providing information on capacitance and ESR. These values respect at the same time time-constant in automotive applications [16]. The Fig. 9 reports relative ESR and capacitance evolutions during simple calendar ageing test of 3000F SCs at 2.8V and 50°C (mean values of three tested cells). Obtained results (Fig. 9) show that the calendar ageing affects significantly the capacitance and the real part of cell impedance. Moreover, we notice that the ESR and capacitance increase and decrease continuously with ageing. We can also deduce that the capacitance of SCs is more impacted with calendar ageing test than the ESR.

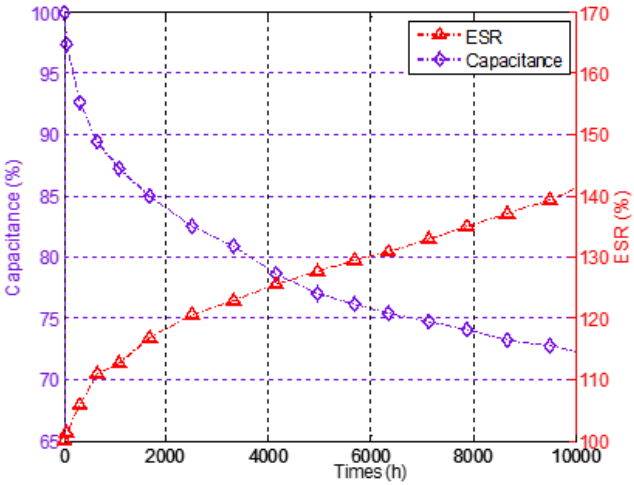

Fig.9 Evolution of capacitance and ESR during Calendar ageing test @2.8V and 50°C

We present now results of the evolution of SCs capacitance and ESR in the case of thermal cycling test. These parameters are both calculated with the same method used previously. Fig. 10 report relative ESR and capacitance evolutions during thermal cycling test at a voltage test of 2.8V and under [40°C-50°C] and [40°C-60°C] temperatures. Mean value of three cells are presented each times. Obtained results highlight a more important degradation rate in the case of thermal cycling than for the calendar ageing made at a constant temperature value. This evolution confirms our observation presented previously in [17]. The decrease of capacitance still more important that the increase of ESR. In addition, according to results presented on Fig.11, for the (40°C-60°C) thermal cycling test for example, the acceleration of degradation rate is very clear when compared to calendar ageing at 50°C.

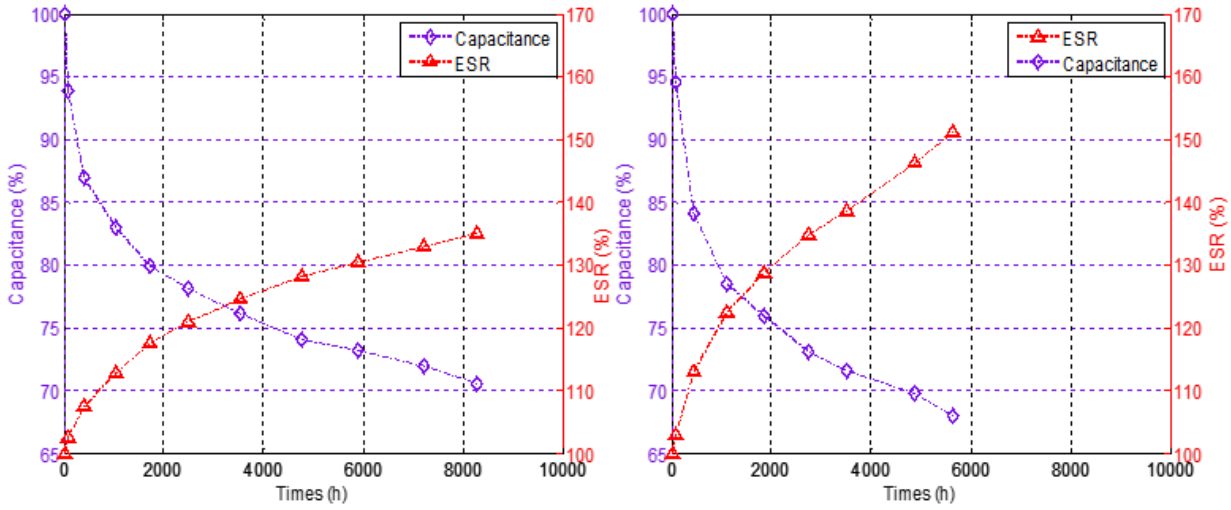

(a) (b)

Fig.10 Evolution of capacitance and ESR during thermal cycling test @2.8V and 40/50°C (a), 2.8V and 40/60°C (b)

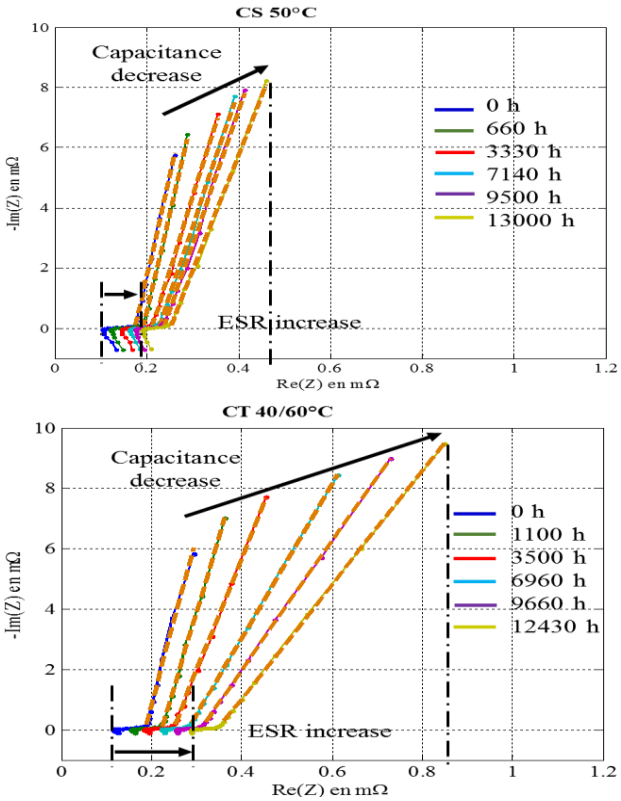

Fig.11 Evolution of Nyquist impedance diagram under calendar ageing without and with thermal cycling

B. Results Comparison and Discussion

In order to understand more the observed behavior of SCs aged in the case of thermal cycling compared to simple calendar ageing test, a comparison method based on parameters modelling study is used to show internal physical parameters change between the two kinds of tests. For the CPE and the MP models, normalized modelling parameters of calendar and thermal cycling ageing tests are grouped and presented as a function of ageing time in Fig.12, which allow us comparing and deducing hypothesis on ageing mechanisms.

The temperature is a very important factor that affects many phenomena inside the SC. As R_s is the sum of the current collectors, the terminals and the separator resistances, its values depends on the quality of the polymer materials used for bind the electrode structure around the collector, its increase could be a direct result of binder decomposition by redox reaction [18]. According to obtained results, thermal cycling between 40 and 60°C accelerate the rate of internal reaction which are the principle responsible of the degradation of porous carbon structure compared to calendar ageing at 50°C. The evolution of calculated time constant of each branch ($R_{eli}.C_{dli}$) (in the MP model), witch present different group of pores in the porous structure, confirm also this conclusion. The increase in the required time to reach the pores shown in Fig. 12 (b) confirms that we have more obstacles in the porous structure in the case of thermal cycling.

For capacitance loss, results show that different trends of decrease have been obtained. The more important loss is observed for the thermal cycling test. The origin of capacitance loss comes essentially because of decomposition reactions of impurities that produce a loss of porous activated carbon surface. We estimate that switching temperature result a thermodynamic equilibrium move and so an increase of internal reaction rate and consequently an acceleration of capacitance decrease. For the R_{el} parameter, we do not detect a significant change. This parameter characterizes the ability of ions to move inside porous structure. So the rise of time constant is related to the diminution of accessible pores number and not to the ions mobility. Slow variations of the γ parameter are also observed. This parameter depends on the dispersion of pores size. Due to the long duration of our ageing tests, an increase of his evolution can be observed. According to presented results, a significant increase is calculated for the 40-60°C thermal cycling test. Therefore, an important change in the pores size is occurred compared to simple calendar ageing results at the mean temperature (50°C). The increase of the time constants also observed, confirms this conclusion.

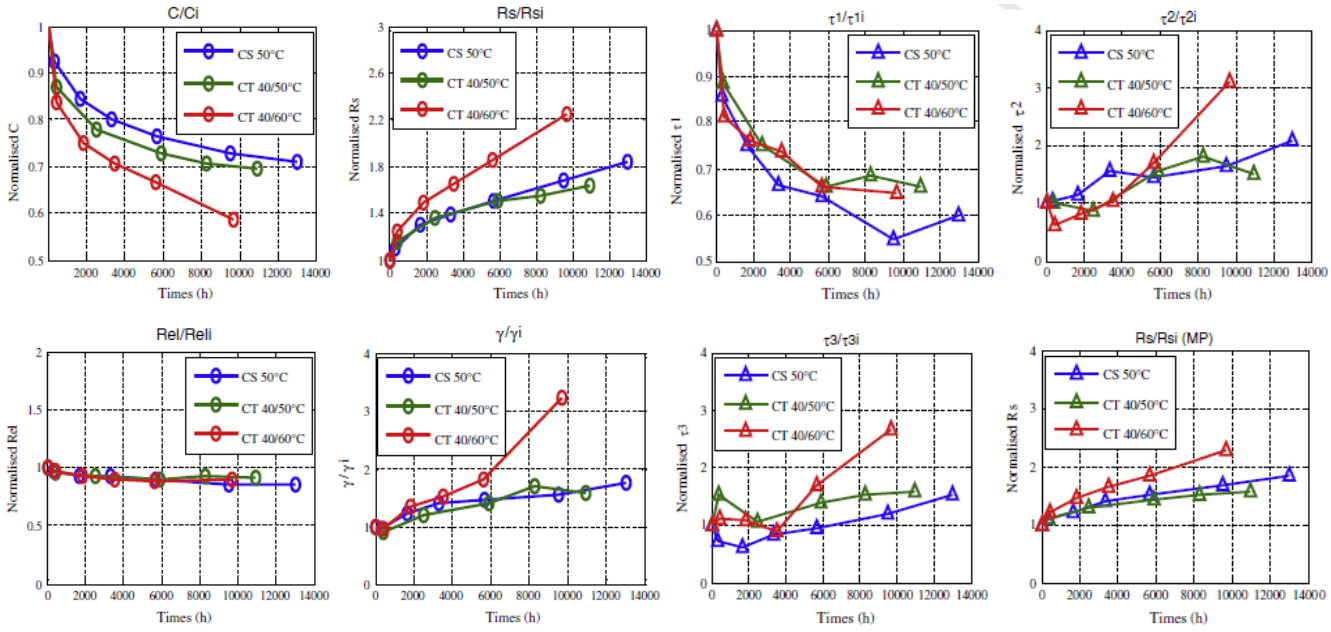

(a) (b)

Fig.12 Comparison between normalized modeling parameters for simple calendar ageing and thermal cycling tests @2.8V and 50°C, 40/50°C, 40/60°C; (a) :CPE model, (b) :MP model

VII. CONCLUSION

This work show the impacts caused by thermal cycling on measured leakage current and supercapacitors performances compared to simple calendar ageing test. A study of temperature on leakage current has been presented. A comparison method based on the study of modelling parameters delivered from two physical models (CPE and MP) has been used to show the internal physical change between the two kinds of ageing tests. Acceleration in ageing rate due to thermal cycling was observed compared to a calendar-ageing test at the same voltage and under the mean value of used temperatures. This confirms that the temperature is an important factor that can affect behavior of used devices.

ACKNOWLEDGMENT

These researches are performed in the “SUPERCAL” project. This project is financed by French national research agency (ANR) and it is a partnership between three scientific laboratories: IMS (in Bordeaux), LTN-IFSTTAR (in Versailles-Satory), Ampère (in Lyon), and three manufacturers from transportation and energy storage devices sectors (PSA Peugeot Citroën, Blue Solutions, Valeo).

REFERENCES

[1] P. Sharma and T. Bhatti, “A review on electrochemical double-layer capacitors”, Energy Conversion and Management, vol. 51, no. 12, pp. 2901 – 2912, 2010.
[2] N. Devillers, S. Jemei, M-C. Péra, D. Bienaimé and F. Gustin, “Review of characterization methods for supercapacitor modelling”, Journal of Power Sources, vol. 246, pp. 596 – 608, 2014.
[3] D. Pankratov, P. Falkman, Z. Blum and S. Shleev, “A hybrid electric power device for simultaneous generation and storage of electric energy”, Energy Environmental Science, vol. 7, pp. 989, 2014.
[4] M. Ayadi, A. Eddahech, O. Briat, J.-M. Vinassa, “Voltage and temperature impacts on leakage current in calendar ageing of supercapacitors,” Fourth International Conference on Power Engineering, Energy and Electrical Drives (POWERENG), pp. 1466 – 1470, 2013.
[5] R. Kötz, P. Ruch, and D. Cericola, “Ageing and failure mode of electrochemical double layer capacitors during accelerated constant load tests”, Journal of Power Sources, vol. 195, no. 3, pp. 923 – 928, 2010.
[6] N. Devillers, S. Jemei, M.C. Péra, D. Bienaimé, F. Gustin, “Review of characterization methods for supercapacitor modelling”, Journal of Power Sources, vol. 246, pp. 596–608, 2014.
[7] S.M. Lambert, V. Pickert, J. Holden, X He, W Li, “Comparison of supercapacitor and lithium-ion capacitor technologies for power electronics applications”, 5th IET International Conference on Power Electronics, Machines and Drives (PEMD 2010), pp.1-5, 2010.
[8] W. Lajnef, J.-M. Vinassa, O. Briat, S. Azzopardi, E. Woirgard, “Characterisation methods and modelling of ultracapacitors for use as peak power sources”, Journal of Power Sources, vol. 168, pp. 553–560, 2007.
[9] S. Fletcher, F. Sillars, R. Carter, A. Cruden, M. Mirzaeian, N. Hudson, J. Parkinson, and P. Hall, “The effects of temperature on the performance of electrochemical double layer capacitors”, Journal of Power Sources, vol. 195, no. 21, pp. 7484 – 7488, 2010.
[10] A. Lewandowski, P. Jakobczyk, M. Galinski, “Capacitance of electrochemical double layer capacitors”, Electrochimica Acta, vol. 86, pp. 225, 2012.

[11] S. Yamazaki, A. Takegawa, Y. Kaneko, J.-I Kadokawa, M. Yamagata and M. Ishikawaa, “Performance of Electric Double-Layer Capacitor with Acidic Cellulose–Chitin Hybrid Gel Electrolyte”, Journal of the Electrochemical Society, vol. 157, no. 2, pp. A203-A208, 2010.
[12] R. Kotz, M. Hahna and R. Gallay, “Temperature behavior and impedance fundamentals of supercapacitors”, Journal of Power Sources, vol. 154, pp. 550 – 555, 2006.
[13] X. Zhang, X. Wang, L. Jiang, H. Wu, C. Wu, and J. Su, “Effect of aqueous electrolytes on the electrochemical behaviors of supercapacitors based on hierarchically porous carbons”, Journal of Power Sources, vol. 216, pp. 290 – 296, 2012.
[14] S. Buller, E. Karden, D. Kok, RW. De Doncker, “Modeling the dynamic behavior of supercapacitors using impedance spectroscopy”, IEEE Transactions on Industry Applications Society, vol. 38, no. 6, pp. 1622-26, 2002.
[15] A. Hammar, P. Venet , R. Lallemand, G. Coquery, G. Rojat “Study of accelerated aging of supercapacitors for transport applications”, IEEE trans on Industrial Electronics, vol. 57, pp.1473–1478, 2010.
[16] A. Eddahech, O. Briat, M. Ayadi, J.-M. Vinassa, “Modeling and adaptive control for supercapacitor in automotive applications based on artificial neural networks”, Journal of Electric Power Systems Research, vol. 106, pp. 134-41, 2014
[17] M. Ayadi, O. Briat, A. Eddahech, R. German, G. Coquery, J.M. Vinassa, “Thermal cycling impacts on supercapacitor performances during calendar ageing”, Microelectronics Reliability ,vol. 53, no. 9/1, pp. 1628–1631, 2013.
[18] M. Deschamps, E. Gilbert, P. Azais, E. Raymundo-Pinero, M. Ammar, P. Simon, D. Massiot, and F. Béguin, “Exploring electrolyte organization in supercapacitor electrodes with solid-state NMR”, Nature Materials, 2013.